ACTA ASTRONOMICA
Vol. **50** (2000) pp. 369–380

Empirical Luminosities and Radii of Early-Type Stars after Hipparcos[1]

by

M. Jerzykiewicz and J. Molenda-Żakowicz

Wrocław University Observatory, Kopernika 11, 51-622 Wrocław, Poland
e-mail: (mjerz,molenda)@astro.uni.wroc.pl

Received August 19, 2000

ABSTRACT

Using Hipparcos parallaxes we derive empirical luminosities and radii of the early-type stars for which the effective temperatures are known from directly measured angular diameters and total absolute fluxes. The empirical luminosities allow a direct comparison of the position of these stars in the fundamental HR diagram with evolutionary tracks. The comparison shows an overall agreement with the $Y = 0.30$ and $Z = 0.02$ tracks computed with OPAL opacities and moderate amount of overshooting from the convective core. In addition, we present evidence that systematic errors of the masses read off the evolutionary tracks are below 10%. Consequently, the surface gravities obtained from these "evolutionary" masses and the empirical radii are very nearly model-independent. Spectrographic and photometric observations of these stars can therefore be used for verifying model atmospheres and calibrating photometric $\log g$ indices.

Key words: *Stars: early type – Stars: fundamental parameters – Hertzsprung-Russell (HR) and C-M diagrams*

1. Introduction

By "empirical" we mean "derived from directly observed quantities". Thus, the empirical luminosity of a star would be given by

$$L/\mathrm{L}_{\odot} = 31280\, f/\pi^2 \tag{1}$$

where f is the total absolute flux above the Earth's atmosphere and π is the star's parallax. The coefficient in Eq. (1) was computed for f expressed in 10^{-6} erg/cm^2/s, π in milliarcseconds (mas), and the solar constant equal to 1.360×10^6 erg/cm^2/s (Allen 1973). Likewise, the empirical radius would be

$$R/\mathrm{R}_{\odot} = 107.5\,\theta/\pi \tag{2}$$

[1]Based on data obtained with the ESA Hipparcos satellite.

where θ is the star's angular diameter, expressed in the same units as the parallax. Finally, the empirical effective temperature can be defined as

$$T_{\rm eff} = 7402\, f^{\frac{1}{4}}/\theta^{\frac{1}{2}} \qquad (3)$$

with θ expressed in mas.

For 32 stars in the spectral range O5f to F8, which had their angular diameters measured by Hanbury Brown *et al.* (1974) with the Narrabri intensity interferometer, Code *et al.* (1976), henceforth CDBH, have obtained the total absolute fluxes by combining OAO-2 UV spectrophotometry with the ground based visual and infrared observations. CDBH used these data to derive the empirical effective temperatures, establishing the $T_{\rm eff}$ scale for early-type stars that has not been significantly revised since (Crowther 1997, Smalley and Dworetsky 1995, Beeckmans 1977).

At the time, reliable trigonometric parallaxes were available for 12 of the 32 stars. In addition, one star, Spica, which is a double-lined spectroscopic binary and an interferometrically resolved double, had accurately determined distance from a combination of spectrographic and interferometric data (Herbison-Evans *et al.* 1971). Thus, for these 13 stars CDBH could derive the empirical luminosities and radii. CDBH then plotted the 13 stars in an HR diagram with $\log T_{\rm eff}$ and $\log L/{\rm L}_\odot$ as coordinates. In this fundamental HR diagram, all stars earlier than A0 – except the primary component of Spica (B1 IV) – had the standard deviation of $\log L/{\rm L}_\odot$ greater than 0.20. It is therefore not surprising that CDBH did not attempt further analysis such as, *e.g.*, a comparison with theoretical evolutionary tracks.

Publication of the final results of the Hipparcos mission (ESA 1997) has changed the situation in two ways. First, most CDBH stars have now reliable trigonometric parallaxes. Second, for 21 of them, including ten B-type stars, the accuracy of the parallaxes is such that their luminosities can be derived to better than 0.10 dex.

In Section 2 we compute the luminosities and radii of CDBH stars, taking into account the Lutz-Kelker bias. In Section 3 we plot these stars in the fundamental HR diagram, compare their location with evolutionary tracks, and derive and discuss the evolutionary masses and surface gravities. Section 4 contains a summary.

2. The Luminosities and Radii

2.1. The Uncorrected Data

In Table 1 we give the logarithms of the luminosities and radii of the 32 CDBH stars, computed by means of Eqs. (1) and (2) from the total absolute fluxes and angular diameters from Tables 6 and 1 of CDBH and the parallaxes from the *Hipparcos Catalogue* (ESA 1997). The standard deviations of $\log L/{\rm L}_\odot$ and $\log R/{\rm R}_\odot$, also given in Table 1, were computed from the standard deviations of f, θ and π in two steps. First, assuming propagation of errors, we computed standard deviations of $L/\mathrm{L}_\odot$ and $R/\mathrm{R}_\odot$ from the equations:

$$\sigma_L = \frac{31280}{\pi^2}\sqrt{\sigma_f^2 + \left(\frac{2f}{\pi}\right)^2 \sigma_\pi^2}, \tag{4}$$

and

$$\sigma_R = \frac{107.5}{\pi}\sqrt{\sigma_\theta^2 + \frac{\theta^2}{\pi^2}\sigma_\pi^2} \tag{5}$$

which follow from Eqs. (1) and (2), respectively. Second, from the approximate relation $\sigma_{\log X} \approx 0.434\sigma_X/X$ we obtained $\sigma_{\log L}$ and $\sigma_{\log R}$.

In the last column of Table 1 we also list $\log T_{\mathrm{eff}}$, where T_{eff} is from Table 6 of CDBH.

Five stars in Table 1, indicated with an asterisk in column 2, have companions bright enough to affect the measured fluxes. CDBH took this into account, so that the data given in the table are for the primary component. In case of # 16 = γ^2 Vel, the primary component is the O9 I star.

2.2. The Lutz-Kelker Corrections

It is well known that because of random errors, the observed parallaxes are larger, on the average, than the true parallaxes. Hence, absolute magnitudes calculated from the observed parallaxes will be systematically too large (Trumpler and Weaver 1953). Assuming uniform distribution of stars in space and a Gaussian distribution of the observed parallax about the true parallax, Lutz and Kelker (1973) have shown that this systematic effect depends only upon the ratio σ_π/π, where π is the observed parallax. They also derived the correction, ΔM_V, which should be added to the absolute magnitude in order to remove the effect. The correction quickly decreases with σ_π/π: for $\sigma_\pi/\pi = 0.050$, $\Delta M_V = -0.02$ mag, for $\sigma_\pi/\pi = 0.100$, $\Delta M_V = -0.11$ mag, and for $\sigma_\pi/\pi = 0.175$, $\Delta M_V = -0.43$ mag. For $\sigma_\pi/\pi > 0.175$, the correction becomes indeterminate.

The luminosities and radii computed from the observed parallaxes by means of Eqs. (1) and (2) will also need correcting for the Lutz-Kelker (L-K) bias. The L-K correction to $\log L/\mathrm{L}_\odot$ will be $\Delta\log L = -\Delta M_V/2.5$, and the correction to $\log R/\mathrm{R}_\odot$ will be $\Delta\log R = -\Delta M_V/5$. In what follows we shall use the interpolation formula

$$\Delta M_V = 5\log\{[1+\sqrt{1-19(\sigma_\pi/\pi)^2}]/2\} \tag{6}$$

provided by Smith (1987).

The CDBH stars are all brighter than $B \approx 2.5$ mag, the limiting magnitude of the Narrabri intensity interferometer. Since luminous stars tend to have small parallaxes, the largest $\log L/\mathrm{L}_\odot$ in Table 1 have the largest standard deviations. This can be also seen from Fig. 1, where $\log L/\mathrm{L}_\odot$ are plotted as a function of relative accuracy of the Hipparcos parallax, σ_π/π. The two vertical dashed lines, at $\sigma_\pi/\pi = 0.050$ and 0.175 have the following significance: (1) to the left of the

Table 1

The empirical luminosities, radii and effective temperatures of CDBH stars; the luminosities and radii are uncorrected for the L-K bias

#	Name	HIP	MK	$\log L/L_\odot$	$\log R/R_\odot$	$\log T_{\rm eff}$ [K]
1	α Eri	7588	B3 Vp	3.520 ± 0.041	0.959 ± 0.019	4.162 ± 0.012
2	β Ori	24436	B8 Ia	4.830 ± 0.168	1.813 ± 0.084	4.063 ± 0.006
3	γ Ori	25336	B2 III	3.815 ± 0.075	0.761 ± 0.040	4.334 ± 0.016
4	ε Ori	26311	B0 Ia	5.504 ± 0.328	1.485 ± 0.165	4.395 ± 0.016
5	ζ Ori*	26727	O9.5 Ib	5.082 ± 0.198	1.112 ± 0.093	4.476 ± 0.031
6	κ Ori	27366	B0.5 Ia	4.700 ± 0.160	1.029 ± 0.079	4.421 ± 0.021
7	β CMa	30324	B1 II-III	4.424 ± 0.106	0.932 ± 0.051	4.401 ± 0.020
8	α Car	30438	F0 Ib-II	4.112 ± 0.047	1.833 ± 0.057	3.873 ± 0.027
9	γ Gem	31681	A0 IV	2.184 ± 0.067	0.681 ± 0.043	3.967 ± 0.014
10	α CMa	32349	A1 V	1.396 ± 0.017	0.223 ± 0.012	3.999 ± 0.007
11	ε CMa	33579	B2 II	4.355 ± 0.074	1.055 ± 0.042	4.322 ± 0.016
12	δ CMa	34444	F8 Ia	4.754 ± 0.268	2.328 ± 0.147	3.786 ± 0.031
13	η CMa	35904	B5 Ia	5.247 ± 0.486	1.898 ± 0.245	4.124 ± 0.018
14	α CMi	37279	F5 IV-V	0.840 ± 0.018	0.315 ± 0.013	3.814 ± 0.009
15	ζ Pup	39429	O5f	5.578 ± 0.207	1.287 ± 0.100	4.512 ± 0.026
16	γ^2 Vel*	39953	WC8+O9 I	5.175 ± 0.150	1.086 ± 0.077	4.512 ± 0.034
17	β Car	45238	A1 IV	2.349 ± 0.021	0.765 ± 0.020	3.966 ± 0.010
18	α Leo	49669	B7 V	2.391 ± 0.030	0.544 ± 0.021	4.087 ± 0.011
19	β Leo	57632	A3 V	1.143 ± 0.018	0.200 ± 0.033	3.947 ± 0.017
20	γ Crv	59803	B8 III	2.555 ± 0.044	0.610 ± 0.039	4.095 ± 0.018
21	β Cru*	62434	B0.5 III	4.566 ± 0.086	0.924 ± 0.032	4.441 ± 0.018
22	α Vir*	65474	B1 IV	4.223 ± 0.076	0.876 ± 0.036	4.379 ± 0.015
23	ε Cen	66657	B1 III	4.146 ± 0.097	0.774 ± 0.047	4.411 ± 0.020
24	δ Sco*	78401	B0.5 IV	4.515 ± 0.122	0.784 ± 0.060	4.498 ± 0.027
25	ζ Oph	81377	O9.5 V	4.744 ± 0.112	0.886 ± 0.061	4.504 ± 0.028
26	α Oph	86032	A5 III	1.369 ± 0.019	0.399 ± 0.035	3.904 ± 0.018
27	ε Sgr	90185	A0 V	2.532 ± 0.043	0.837 ± 0.027	3.976 ± 0.010
28	α Lyr	91262	A0 V	1.757 ± 0.018	0.431 ± 0.010	3.985 ± 0.006
29	α Aql	97649	A7 IV-V	1.003 ± 0.017	0.217 ± 0.021	3.904 ± 0.011
30	α Pav	100751	B2.5 V	3.333 ± 0.051	0.684 ± 0.032	4.252 ± 0.016
31	α Gru	109268	B7 IV	2.611 ± 0.036	0.533 ± 0.032	4.148 ± 0.017
32	α PsA	113368	A3 V	1.211 ± 0.016	0.239 ± 0.029	3.944 ± 0.015

first line the L-K corrections to $\log L/L_\odot$, $\Delta \log L \leq 0.008$, *i.e.*, they are not greater than half the smallest $\sigma_{\log L}$ in Table 1, (2) to the right of the second line, the corrections become indeterminate. As can be seen from Fig. 1, all but two CDBH stars with $\log L/L_\odot < 4.0$ will have $\Delta \log L \leq 0.008$, while the correction will be indeterminate for six stars, all with $\log L/L_\odot > 4.5$.

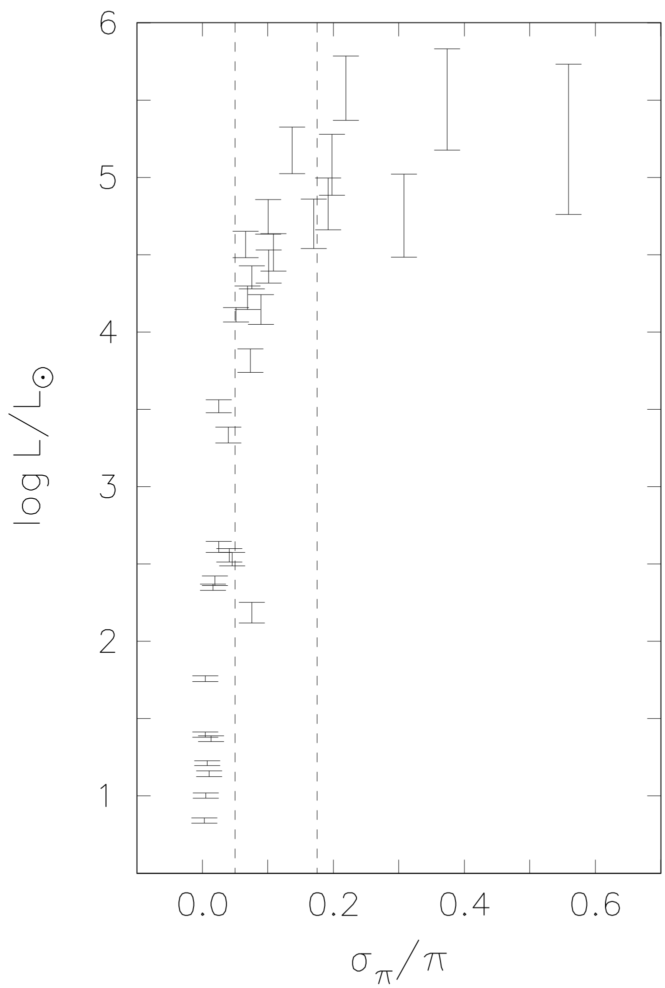

Fig. 1. Logarithmic luminosities of the 32 CDBH stars, shown as a function of relative accuracy of the Hipparcos parallax. In order to avoid crowding, only the error bars are plotted; they are equal to twice the standard deviations of $\log L/\mathrm{L}_\odot$ (see Table 1). The vertical dashed lines indicate $\sigma_\pi/\pi = 0.05$ and 0.175. The significance of these numbers is explained in the text.

3. Discussion

3.1. The Fundamental HR Diagram

CDBH stars are shown in the fundamental HR diagram in Figs. 2 and 3; the stars with $\log L/\mathrm{L}_\odot < 4.0$ are plotted in Fig. 2, while those with $\log L/\mathrm{L}_\odot > 4.0$, in Fig. 3. In both figures, $\log T_{\mathrm{eff}}$ is used as abscissa and $\log L/\mathrm{L}_\odot + \Delta\log L$ as ordinate, where $\log T_{\mathrm{eff}}$ and $\log L/\mathrm{L}_\odot$ are from Table 1 and $\Delta\log L = -\Delta M_V/2.5$, with ΔM_V given by Eq. (6). The stars are identified in the figures with the numbers from the first column of Table 1. In Fig. 2, the stars shown with the large filled circles have $\Delta\log L \leq 0.008$ (see the preceding Section); the two stars plotted as small filled circles with error bars have $\Delta\log L = 0.024$. In Fig. 3, the crossed error bars indicate uncorrected luminosities from Table 1. In this figure, the L-K corrections range from 0.011 for # 8 = αCar to 0.156 for # 6 = κOri. For six stars, β, ε and ζ Ori, δ and η CMa, and ζ Pup, the correction is indeterminate.

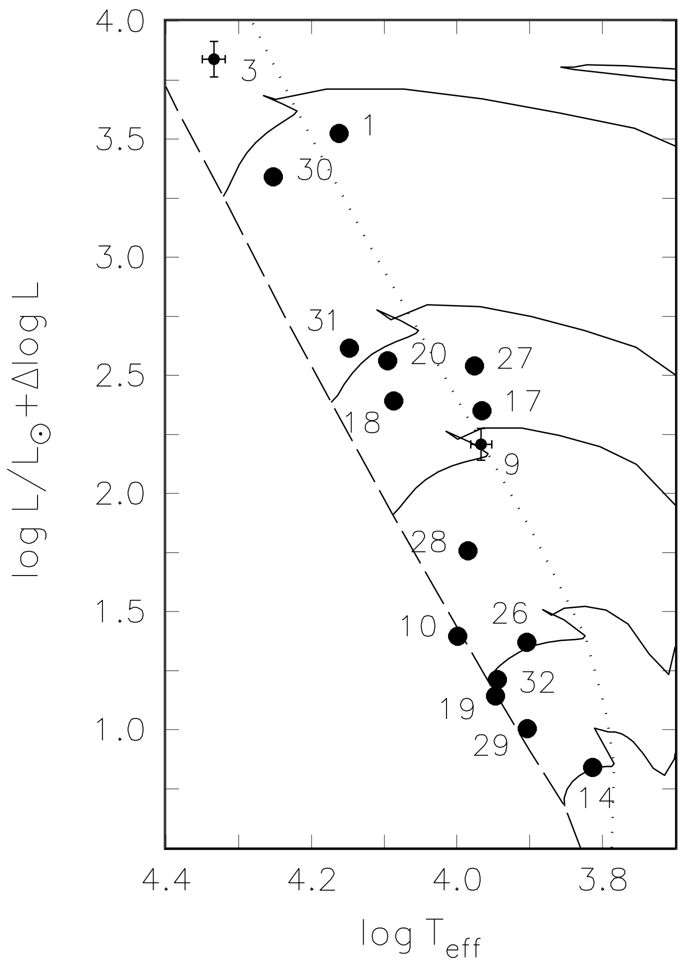

Fig. 2. Fundamental HR diagram for CDBH stars with $\log L/\mathrm{L}_\odot < 4.0$. Stars with the Lutz-Kelker correction, $\Delta\log L$, not greater than 0.008 are plotted as large filled circles, while two stars with $\Delta\log L = 0.024$ are shown as small filled circles with error bars, where the error bars are twice the standard deviations of $\log T_{\mathrm{eff}}$ and $\log L/\mathrm{L}_\odot$ from Table 1. For the large filled circles the error bars were omitted because they would seldom extend beyond the plotted symbol. Also shown are the $Y = 0.30$, $Z = 0.02$ evolutionary tracks from Schaller *et al.* (1992) for initial masses of 1.5, 2, 3, 4 and 7 $\mathrm{M}_\odot$ (solid lines); the tracks define theoretical ZAMS and TAMS (the dashed and dotted line, respectively).

The evolutionary tracks plotted in Figs. 2 and 3 are the $Y = 0.30$, $Z = 0.02$ ones from Schaller *et al.* (1992). These authors use the opacity tables of Rogers and Iglesias (1992) and they adjust Y to match the solar luminosity and age. For masses greater than 1.25 $M_\odot$ they include overshooting from the convective core, assuming the overshooting parameter to be equal to 0.2 times the pressure scale height, mainly in order to fit the observed upper envelope of the main-sequence of a number of open clusters and associations.

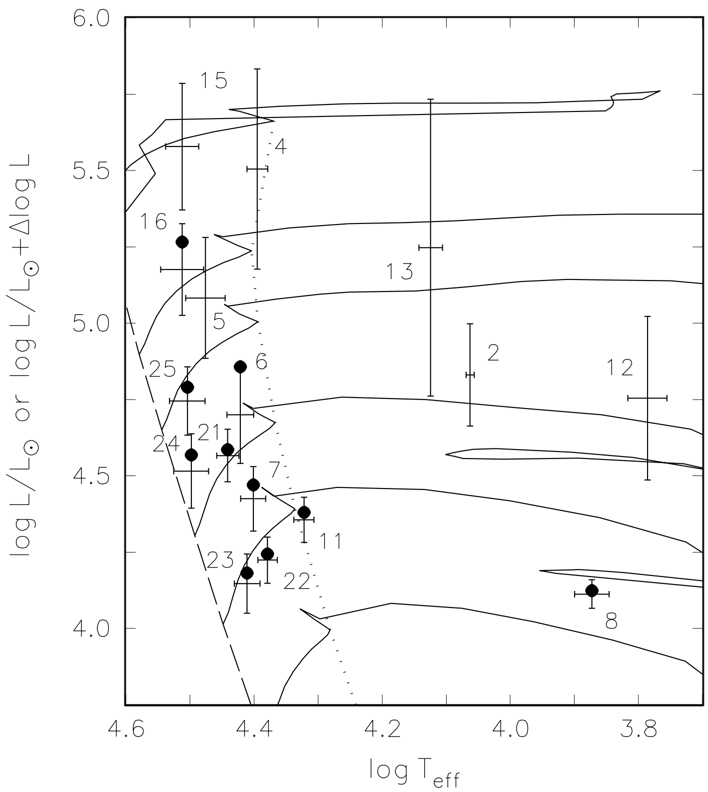

Fig. 3. Fundamental HR diagram for CDBH stars with $\log L/\mathrm{L}_\odot > 4.0$. Crossed error bars indicate uncorrected positions, with $\log L/\mathrm{L}_\odot$ from Table 1 as ordinates, while filled circles have ordinates corrected for the L-K effect, $\log L/\mathrm{L}_\odot + \Delta \log L$. Also plotted are the $Y = 0.30$, $Z = 0.02$ evolutionary tracks from Schaller *et al.* (1992) for initial masses of 9, 12, 15, 20, 25 and 40 $M_\odot$ (solid lines) and the theoretical ZAMS and TAMS they define (the dashed and dotted line, respectively).

In Figs. 2 and 3, most stars with reliable luminosities (*i.e.,* those for which the L-K correction could be derived) lie in the regions of slow nuclear burning, either in the theoretical main-sequence band (22 stars) or in the area of core-He burning (# 8 = αCar). Only three stars, all in Fig. 2, viz., # 1 = αEri, # 17 = βCar and # 27 = εSgr, are found in the Hertzsprung gap, where the theory predicts evolution on thermal time-scale. However, they are all rather close to the TAMS line. Shifting this line to lower temperatures by increasing the overshooting parameter or taking into account rotation (Fliegner and Langer 1994, Breger and Pamyatnykh 1998), so that the three stars would be included within the main-sequence band, is probably not beyond uncertainties of the models. Rotation may be important especially in the case of α Eri for which the projected rotation velocity amounts to 250 km/s (Hoffleit 1982). Another possibility is that these stars have Z somewhat higher than 0.02, say 0.03. In any case, the position of the CDBH stars in the fundamental HR diagram is not in conflict with standard evolutionary calculations which include moderate amount of core-overshooting. Note that this conclusion is independent of any photometric or spectrographic calibrations, because no calibrations of this sort have been used here. Thus, changing Z, for instance, does not affect the observed position of these stars in the HR diagram. Finally, the conclusion would be unchanged if we used other recent models with similar initial chemical composition and moderate overshooting, for example, those of Claret and Giménez (1992) or Dziembowski and his co-workers (Pamyatnykh *et al.* 1998).

3.2. Evolutionary Masses and Surface Gravities

Given a star's position in the fundamental HR diagram, its mass can be read off the evolutionary track. Masses obtained in this way are usually qualified with the adjective "evolutionary." For the 25 CDBH stars with reliable luminosities, the evolutionary masses obtained from the $Y = 0.30$, $Z = 0.02$ evolutionary tracks of Schaller *et al.* (1992) are listed in the third column of Table 2. In most cases core-hydrogen-burning segments of the tracks were used; if not, a remark in the last column is provided. For #6 = κOri, #8 = αCar, #9 = γGem and #11 = εCMa, which lie in the regions where the tracks intersect each other, the largest and the smallest value of the mass is given. The mean errors of the masses were estimated from the mean errors of the luminosities, using the theoretical mass-luminosity relations parallel to the ZAMS relation and passing through the point in question.

For Sirius A and Procyon A (#10 and #14 in Fig. 2), and Spica A (#22 in Fig. 3), the evolutionary masses can be compared with the empirical ones, known from orbital solutions. The empirical masses amount to 2.143 ± 0.056 $M_\odot$ for Sirius A (Gatewood and Gatewood 1978), 1.751 ± 0.051 and 1.497 ± 0.037 $M_\odot$ for Procyon A (Irwin *et al.* 1992 and Girard *et al.* 2000, respectively), and 10.9 ± 0.9 $M_\odot$ for Spica A (Herbison-Evans *et al.* 1971). For Sirius A and Spica A, the agreement is at the 1.5 sigma and below one sigma level, respectively. In the case of Procyon A, the conflict of the higher empirical mass value with the evolutionary one has been known for a long time. Girard *et al.* (2000) derived the lower mass value, in perfect agreement with the evolutionary one, from an astrometric solution in which they gave high weight to the measurement of the primary–white dwarf separation obtained by means of the Planetary Camera on the Hubble Space Telescope.

The differences between the evolutionary and empirical masses amount to 4% for Sirius A, 15 and 1% for Procyon A, and 5% for Spica A. Note that the evolutionary masses are all greater than the empirical ones. Whether this is an indication of a systematic effect or a fluke of small number statistics is impossible to say. In any case, it is probably safe to assume that systematic errors of the evolutionary masses in Table 2 are below 10%.

T a b l e 2

Evolutionary masses and surface gravities of 25 CDBH stars with reliable luminosities

#	Name	$M/\mathrm{M}_\odot$	$\log g$	Remarks
1	α Eri	6.22 $\pm$ 0.16	3.31 $\pm$ 0.04	SHB
3	γ Ori	8.88 $\pm$ 0.45	3.84 $\pm$ 0.085	
6	κ Ori	17.7 $\pm$ 2.3	3.47 $\pm$ 0.17	
6		16.4 $\pm$ 2.1	3.44 $\pm$ 0.17	SHB
7	β CMa	13.5 $\pm$ 1.1	3.66 $\pm$ 0.11	
8	α Car	9.97 $\pm$ 0.33	1.68 $\pm$ 0.12	1st crossing
8		8.33 $\pm$ 0.24	1.76 $\pm$ 0.12	3rd crossing
9	γ Gem	2.89 $\pm$ 0.10	3.51 $\pm$ 0.09	SHB
9		3.07 $\pm$ 0.11	3.54 $\pm$ 0.09	TAMS
10	α CMa	2.23 $\pm$ 0.022	4.340 $\pm$ 0.024	
11	ε CMa	11.8 $\pm$ 0.6	3.37 $\pm$ 0.09	TAMS
11		11.4 $\pm$ 0.6	3.36 $\pm$ 0.09	SHB
14	α CMi	1.51 $\pm$ 0.015	3.984 $\pm$ 0.026	
16	γ^2 Vel*	27.5 $\pm$ 4.4	3.62 $\pm$ 0.18	
17	β Car	3.12 $\pm$ 0.037	3.40 $\pm$ 0.04	SHB
18	α Leo	3.60 $\pm$ 0.062	3.90 $\pm$ 0.04	
19	β Leo	1.93 $\pm$ 0.020	4.33 $\pm$ 0.07	
20	γ Crv	3.89 $\pm$ 0.098	3.80 $\pm$ 0.08	
21	β Cru*	15.2 $\pm$ 1.1	3.75 $\pm$ 0.07	
22	α Vir*	11.5 $\pm$ 0.6	3.73 $\pm$ 0.08	
23	ε Cen	11.8 $\pm$ 0.8	3.93 $\pm$ 0.10	
24	δ Sco*	17.3 $\pm$ 1.8	4.06 $\pm$ 0.13	
25	ζ Oph	19.1 $\pm$ 1.8	3.90 $\pm$ 0.13	
26	α Oph	2.02 $\pm$ 0.021	3.94 $\pm$ 0.07	
27	ε Sgr	3.47 $\pm$ 0.082	3.30 $\pm$ 0.06	SHB
28	α Lyr	2.52 $\pm$ 0.026	3.976 $\pm$ 0.020	
29	α Aql	1.75 $\pm$ 0.017	4.25 $\pm$ 0.04	
30	α Pav	6.34 $\pm$ 0.22	3.87 $\pm$ 0.07	
31	α Gru	4.16 $\pm$ 0.091	3.99 $\pm$ 0.06	
32	α PsA	1.97 $\pm$ 0.018	4.256 $\pm$ 0.015	

* Corrected for duplicity.

Using the evolutionary masses and the empirical radii from Table 1, corrected with $\Delta\log R = -\Delta M_V/5$, where ΔM_V is given by Eq. (6) (see Section 2.2), we computed $\log g$ values for the 25 CDBH stars with reliable luminosities; they are listed in the fourth column of Table 2.

For the sake of illustration, these $\log g$ values are plotted in Fig. 4 as a function of $\log R/\mathrm{R}_\odot$. For αCar, the 3rd crossing value is plotted; for κOri, γGem and εCMa, the core-hydrogen-burning values are shown. Also plotted in Fig. 4 are empirical $\log g$ values, obtained from SB2 eclipsing binaries. These include the data for components of common binaries from Andersen (1991) and those for four well-observed ζAur systems from Griffin *et al.* (1990, 1992, 1993, 1995).

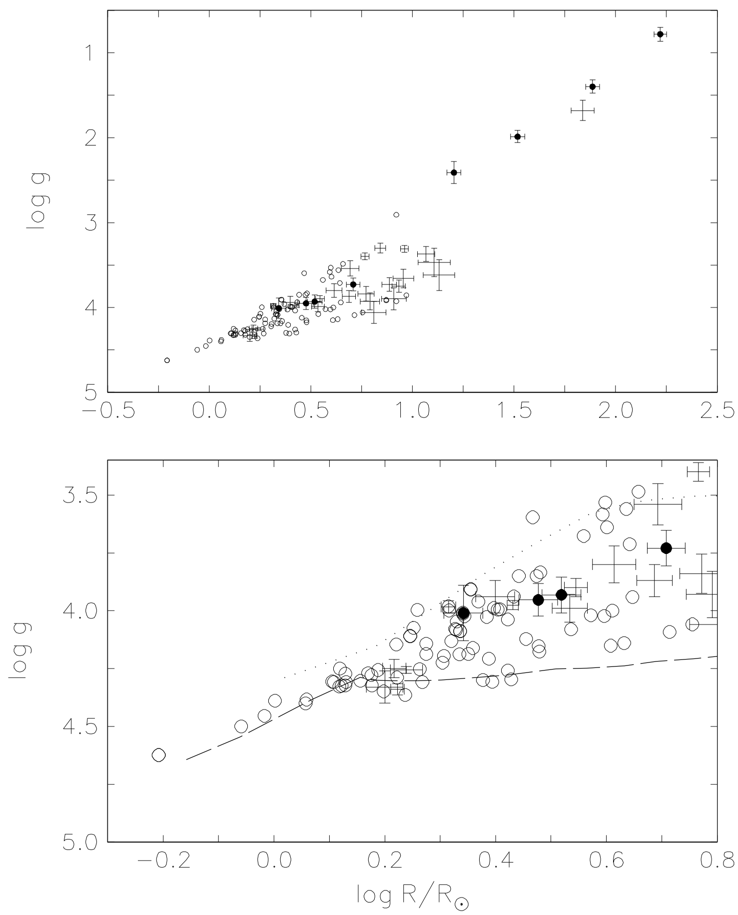

Fig. 4. Comparison of the $\log g$ values of CDBH stars from Table 2 (crossed error bars) with the empirical $\log g$ values. Open circles are components of common eclipsing binaries from Andersen (1991), while points with error bars are components of four ζ Aur systems. The latter, in order of increasing radius of the giant component, are: τ Per (Griffin *et al.* 1992), HR 6902 (Griffin *et al.* 1995), 22 Vul (Griffin *et al.* 1993), and ζ Aur (Griffin *et al.* 1990). The lower panel shows the crowded lower left-hand quadrant of the upper panel. In this panel, the $Y = 0.30$, $Z = 0.02$ ZAMS and TAMS loci, derived from Schaller *et al.* (1992), are also shown (the dashed and dotted line, respectively). For the Andersen's (1991) data, the error bars were omitted because they would seldom extend beyond the plotted symbol.

As can be seen from Fig. 4, our $\log g$ values (crossed error bars) fall in the same area as the empirical ones. This is hardly surprising: since a 10% error in mass translates into an error of barely 0.04 in $\log g$, these values are very nearly model-independent. Now, with their empirical effective temperatures known, the stars of Table 2 become the best objects for verifying model atmospheres. In particular, they can serve as standards in calibrating photometric $\log g$ indices such as β for the B-type stars or c_1 for the F-type stars. Note that in the case of components of eclipsing binaries the situation is diametrically different: model atmospheres or photometric indices are used to derive effective temperatures (Andersen 1991, Schönberner and Harmanec 1995). However, the question of how rotation and metallicity affect the observed spectrum and the photometric indices may require an examination of each CDBH star individually.

4. Summary

For 26 stars with directly determined angular diameters (Hanbury Brown *et al.* 1974) and total absolute fluxes (Code *et al.* 1976), the accuracy of their Hipparcos parallaxes is sufficient for calculating the luminosities and radii with the Lutz-Kelker bias taken into account. Plotted on the fundamental HR diagram, these stars fall in (23 stars) or close to (3 stars) the regions of slow nuclear burning as predicted by the solar composition evolutionary models, computed with OPAL opacities and moderate (0.2 pressure scale height) convective core overshooting.

For these stars, the $\log g$ values, obtained from the evolutionary masses and empirical radii, are very nearly model-independent. Therefore, they can be used as standards for verifying model atmospheres and calibrating photometric $\log g$ indices.

Acknowledgements. This research has made use of NASA's Astrophysics Data System Abstract Service. J.M.-Ż. acknowledges support from the Wrocław University grant 2041/W/IA/1998.

REFERENCES

Allen, C.W. 1973, "Astrophysical Quantities", 3rd ed. London: Athlone Press, p. 169.
Andersen, J. 1991, *Astron. Astrophys. Rev.*, **3**, 91.
Beeckmans, F. 1977, *Astron. Astrophys.*, **60**, 1.
Breger, M., and Pamyatnykh, A.A. 1998, *Astron. Astrophys.*, **332**, 958.
Claret, A., and Giménez, A. 1992, *Astron. Astrophys. Suppl. Ser.*, **96**, 255.
Code, A.D., Davis, J., Bless, R.C., and Hanbury Brown, R. 1976, *Astrophys. J.*, **203**, 417 (CDBH).
Crowther, P.A. 1997, in: "Fundamental Stellar Properties", *Proc. IAU Symp., 189*, Eds. Bedding, T.R., Booth, A.J., and Davis, J., Kluwer, Dordrecht, p. 137.
ESA 1997, "The Hipparcos and Tycho Catalogues", ESA SP-1200.
Fliegner, J., and Langer, N. 1994, in: "Pulsation, Rotation and Mass Loss in Early-Type Stars", *Proc. IAU Symp.*, 162, Eds. Balona, L.A., Henrichs, F.H., and Le Contel, J.M., Kluwer, Dordrecht, p. 147.
Gatewood, G.D., and Gatewood, C.V. 1978, *Astrophys. J.*, **225**, 191.
Girard, T.M., *et al.* 2000, *Astron. J.*, **119**, 2428.
Griffin, R.E.M., Griffin, R.F., Schröder, K.-P., and Reimers, D. 1990, *Astron. Astrophys.*, **234**, 284.
Griffin, R.E.M., Schröder, K.-P., Misch, A., and Griffin, R.F. 1992, *Astron. Astrophys.*, **254**, 289.
Griffin, R.E.M., Hünsch, M., Marshall, K.P., Griffin, R.F., and Schröder, K.-P. 1993, *Astron. Astrophys.*, **274**, 225.
Griffin, R.E.M., Marshall, K.P., Griffin, R.F., and Schröder, K.-P. 1995, *Astron. Astrophys.*, **301**, 217.
Hanbury Brown, R., Davis, J., and Allen, L.R. 1974, *MNRAS*, **167**, 121.
Herbison-Evans, D., Hanbury Brown, R., Davis, J., and Allen, L.R. 1971, *MNRAS*, **151**, 161.

Hoffleit, D. 1982, "The Bright Star Catalogue", Yale University Observatory, New Haven, Connecticut, U.S.A.

Irwin, A.W., *et al.* 1992, *P.A.S.P.*, **104**, 489.

Lutz, T.E., and Kelker, D.H. 1973, *P.A.S.P.*, **85**, 573.

Pamyatnykh, A.A., Dziembowski, W.A., Handler, G., and Pikall, H. 1998, *Astron. Astrophys.*, **333**, 141.

Rogers, F.J., and Iglesias, C.A. 1992, *Astrophys. J. Suppl. Ser.*, **79**, 507.

Schaller, G., Schaerer, D., Meynet, G., and Maeder, A. 1992, *Astron. Astrophys. Suppl. Ser.*, **96**, 269.

Schönberner, D., and Harmanec, P. 1995, *Astron. Astrophys.*, **294**, 509.

Smalley, B., and Dworetsky, M.M. 1995, *Astron. Astrophys.*, **293**, 446.

Smith, H. 1987, *Astron. Astrophys.*, **188**, 233.

Trumpler, R.J., and Weaver, H.F. 1953, "Statistical Astronomy" University of California Press, Berkeley, p. 369.